Theriogenology Wild 7 (2025) 100135

Contents lists available at ScienceDirect

Theriogenology Wild

journal homepage: www.journals.elsevier.com/theriogenology-wild

Evaluating alternatives to flow cytometry for sex-sorting rhinoceros sperm

Louisa A. Rispoli [a,*], Elizabeth Donelan [a], Parker M. Pennington [a,1], Priscilla H. Joyner [b], Terri L. Roth [a]

[a] Center for Conservation and Research of Endangered Wildlife, Cincinnati Zoo and Botanical Garden, 3400 Vine Street, Cincinnati, OH 45220, USA
[b] The Wilds, 14000 International Road, Cumberland, OH 43732, USA

ARTICLE INFO

Keywords:
Ceratotherium simum
Fluorescence-activated cell sorting (FACS)
Magnetic-activated cell sorting (MACS)
Rhinoceros unicornis
Toll-like receptor (TLR)
Zeta potential

ABSTRACT

Effective sperm sex-sorting techniques could be beneficial for managing ex-situ rhinoceros populations. Fluorescence-activated cell sorting (FACS) technology has shown promise but is limited by high cost, long sorting times, and poor compatibility with frozen sperm. This study evaluated two alternative methods for sex-sorting sperm from white (*Ceratotherium simum*; n = 5) and greater one-horned (*Rhinoceros unicornis*; n = 5) rhinoceroses. Thirteen ejaculates (five fresh and eight cryopreserved) were used to assess Toll-like receptor (TLR) activation and magnetic-activated cell sorting (MACS). The TLR method selectively reduces X-bearing sperm motility via a TLR agonist, whereas MACS separates sperm based on Y-bearing sperm having a more positive surface charge than X-bearing sperm. The TLRs were confirmed to be present in rhinoceros sperm, with TLR7 primarily localized to the head region (90–95 %) and TLR8 to the flagellum (~50 %). Activation with a TLR8 ligand reduced velocity ($P = 0.001$) but did not alter the distribution of X- and Y-bearing sperm in the upper and lower swim-up layers ($P = 0.259$). Negatively charged magnetic nanoparticles associated and pulled a portion of sperm to the tube wall when magnetic force was applied, leaving 35–80 % of sperm free in suspension, depending on the treatment conditions. However, no enrichment for X-bearing sperm was observed in the unbound fraction ($P > 0.27$). These results indicate that neither method physically separated X- from Y-bearing rhinoceros sperm under the tested conditions. Nonetheless, the findings provide important foundational data for refining alternative methods for sex-sorting in this species and highlight both the potential and the challenges of applying such methods.

1. Introduction

Building sustainable ex situ rhinoceros (hereafter referred to as rhino) populations is a critical conservation goal and effective sex ratio management plays an important role. Maintaining an appropriate balance between males and females helps to create stable social groupings and enhances breeding opportunities, ultimately contributing to population health and growth [1,2]. While population sex ratios vary across species and over time in North America [3–5], the recent birth trends of black rhinos (*Diceros bicornis michaeli*) suggest a possible return to a male-biased population [3]. Because adult black rhino bulls are typically housed individually, a predominance of males can strain the capacity of managed facilities [6]. In contrast, white (*Ceratotherium simum*) and greater one-horned (*Rhinoceros unicornis*) rhinos have historically exhibited female-skewed populations, and a current management priority for both species is maximizing the number of breeding bulls [4,5]. Achieving the appropriate sex ratio can be difficult for ex-situ facilities that face significant space limitations and must optimize the reproductive output of each rhino without exceeding available resources [6–8].

Artificial insemination with sex-sorted sperm could potentially allow rhino managers to strategically produce imbalanced sex ratios that favor population management goals [9–11]. Over the past 16 years, encouraging progress has been made using a flow cytometry-based technology, fluorescence-activated cell sorting (FACS), to sex-sort rhino sperm [9,10,12]. FACS takes advantage of the DNA content difference between X-bearing (female-producing) and Y-bearing (male-producing) sperm, using a fluorescent DNA stain and flow cytometry to physically separate the two populations (Fig. 1A; [13]). Unfortunately, FACS has several

* Correspondence to: Center for Conservation and Research of Endangered Wildlife (CREW), Cincinnati Zoo & Botanical Garden, 3400 Vine Street, Cincinnati, OH 45220, USA.
E-mail addresses: Elizabeth.Donelan@cincinnatizoo.org (E. Donelan), Parker@colossal.com (P.M. Pennington), pjoyner@thewilds.org (P.H. Joyner), Terri.Roth@cincinnatizoo.org (T.L. Roth).
[1] Present address: Colossal Foundation, 3309 Elm St., Suite 380, Dallas, TX, 75226, USA

https://doi.org/10.1016/j.therwi.2025.100135
Received 7 May 2025; Received in revised form 27 June 2025; Accepted 1 July 2025
Available online 4 July 2025
2773-093X/© 2025 The Authors. Published by Elsevier Inc. This is an open access article under the CC BY-NC-ND license (http://creativecommons.org/licenses/by-nc-nd/4.0/).

drawbacks, including high equipment costs (>$100 K), specialized expertise requirements, and long sorting times [9,13]. Additionally, FACS does not work well on frozen sperm samples [14] and results in considerable sperm loss and reduced viability during the separation process [13,14]. These limitations hinder the widespread adoption of FACS for sex sorting in rhinoceros conservation efforts, particularly in facilities with constrained funding, equipment, and technical capabilities.

To address these challenges, effective sex ratio management in ex-situ conservation requires sorting alternatives that maintain sperm quality, are affordable, and adaptable to the space and resource limitations of many rhino-holding facilities. Two promising techniques for sex-sorting sperm were investigated in this study. One method is the activation of Toll-like receptors 7 and 8 (TLR7, TLR8) to selectively reduce sperm motility. These membrane receptors play a role in immune signaling and are expressed in the sperm of several species [15]. Previous studies with sperm from mice, cattle, goats, and sheep have demonstrated that activating these receptors can differentially affect sperm motility, causing X-bearing sperm to swim more slowly, thereby allowing X- or Y-bearing sperm to be preferentially collected after TLR activation (Fig. 1B; [16–20]). Compared to FACS, TLR activation offers a more cost-effective and straightforward method for sex-sorting sperm without requiring specialized equipment. In addition to TLR activation, we evaluated the magnetic-activated cell sorting (MACS) of rhino sperm based on differential surface charge. Negatively charged magnetic nanoparticles (MNPs) will associate with Y-bearing sperm, which can have a more positive surface charge than X-bearing counterparts [21–23]. When a magnetic field is applied, the MNP-bound Y-bearing sperm are pulled to the tube wall, while the unbound X-bearing sperm remain in suspension and can be collected (Fig. 1C). The MACS methodology is more sperm-friendly than FACS, as it requires less processing time and fewer buffer changes, which may help to maintain sperm viability longer. Studies in domestic species, such as horses, donkeys, and rams, have demonstrated that differences in surface charge (i.e., zeta potential) between X- and Y-bearing sperm can be exploited to preselect the sex of the offspring [24–26].

Therefore, the objectives of this study were to determine the expression and localization of TLR7 and TLR8 in rhino sperm, to assess the impact of TLR activation on sperm motility and its potential to alter sex ratio distribution, and to evaluate if incubating rhino sperm with negatively charged MNPs can selectively enrich for X-bearing sperm. We aimed to identify cost-effective and sperm-friendly alternatives to FACS for managing sex ratios in ex-situ rhino populations. TLR activation and MACS were chosen for their promising results in other species and their potential application to banked frozen sperm [19,22] from genetically valuable males that are no longer available (e.g., deceased), which can

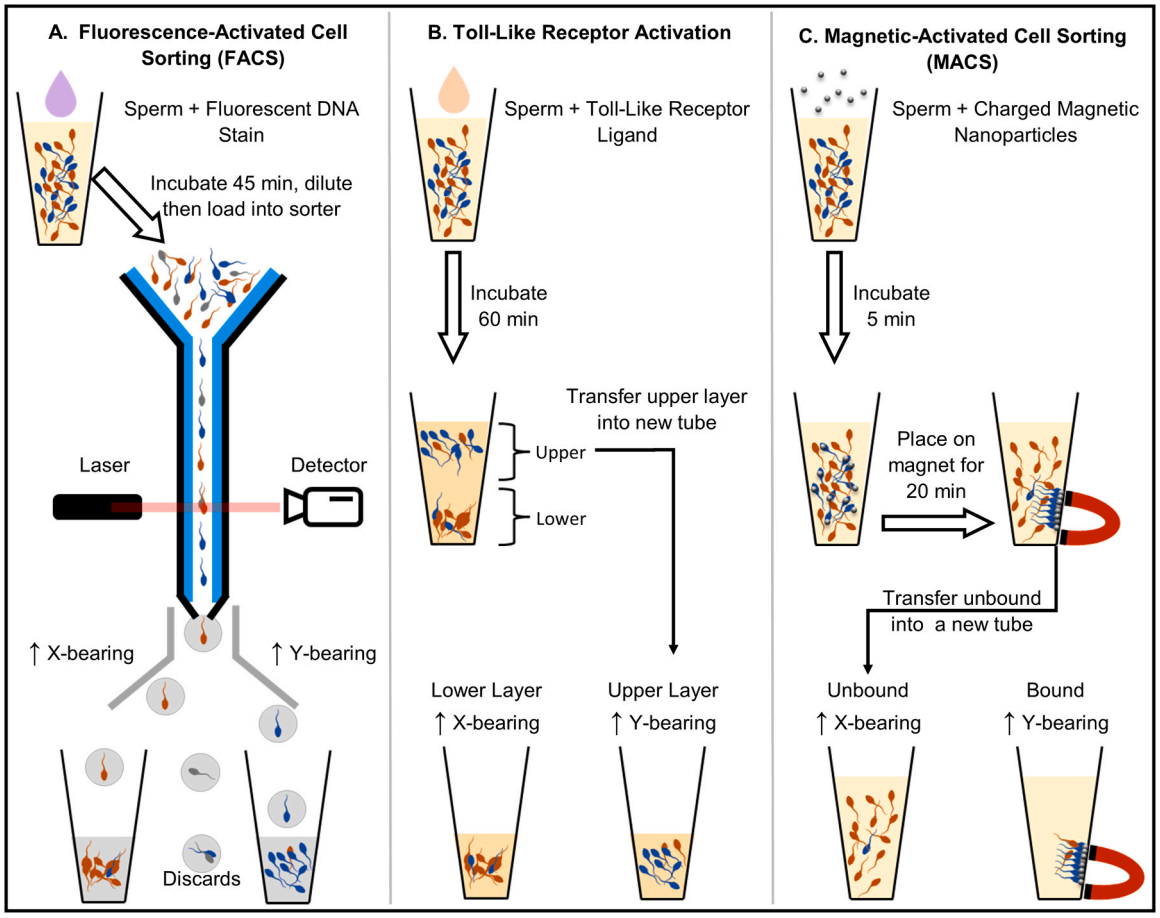

Fig. 1. Schematic representation of sex-sorting methods. In the figure, X-bearing sperm (female-producing) are shown in red and Y-bearing sperm (male-producing) in blue for clarity; grey indicates sperm that cannot be classified. A). Fluorescence-activated cell sorting (FACS) utilizes flow cytometry and a fluorescent DNA stain to differentiate X-bearing sperm (which contain 3–5 % more DNA) from Y-bearing sperm. Droplets containing unclassified or aggregates are discarded. B). Toll-like receptor (TLR) activation occurs after incubating sperm with a TLR ligand, which reduces the motility of X-bearing sperm only, allowing for the preferential collection of Y-bearing sperm that remain motile in the upper layer after the incubation. C). Magnetic-activated cell sorting (MACS) depicted here exploits the difference in zeta potential between Y-bearing sperm (-16 mV) and X-bearing sperm (-20 mV), with Y-bearing sperm more readily associating with the negatively charged magnetic nanoparticles. When a magnetic force is applied, the sperm-MNP complexes are pulled to and anchored against the inner wall of the test tube, while X-bearing sperm remain suspended and can be transferred to a new tube.

be crucial for maintaining genetic diversity in managed rhino populations [27].

2. Materials and methods

2.1. Chemicals and reagents

Unless otherwise noted, chemicals were obtained from MilliporeSigma (St. Louis, MO, USA). Polyclonal antibodies against TLR7 (ab113524, lot GR123749), TLR8 (ab24185, lot GR3368660), and anti-rabbit IgG-AlexaFluor555 conjugate (ab150082) were purchased from Abcam (Cambridge, MA, USA). Synthetic TLR8 ligand (Motolimod, aka VTX-378) was obtained from MedChemExpress LLC (Monmouth Junction, NJ, USA). We sourced charged magnetic nanoparticles (MNPs) in two sizes (50 nm and 100 nm), each coated with a thin diphosphate layer that provided a negative surface charge of −50 mV ± 7 mV (as per personal communication from the company), from Chemicell GmBH (Berlin, Germany). Buffers were prepared according to references and included the following: a modified equine extender (mEQ, pH 7.0–7.2; [10,28]), tris-citrate glucose buffer (TCG, unadjusted pH 7.6; [22,29]), conducting medium (CM, unadjusted pH 5.4; [22,29]), low-conductivity human tubal fluid (LHTF, unadjusted pH 7.2; [29,30]), chamber buffer (CB, pH 7.2; [23]), and modified human tubal fluid (mHTF, pH 7.2–7.4; [26]). Further details on buffer compositions can be found in Supplemental M&M.

2.2. Source of sperm

Sperm samples were originally collected for other purposes under protocols approved by the Cincinnati Zoo and Botanical Garden's Institutional Animal Care and Use Committee (#17–139, #20–163, #22–173, and #22–175) and by each participating zoological institution. The samples were included in this study only after obtaining permission from each owning institution. Sperm from both white (n = 5) and greater one-horned (GOH; n = 5) rhinos were used and included both freshly collected ejaculates (n = 5) and cryopreserved samples (n = 8). Cryopreserved samples had been extended in either an egg yolk-based extender or OptiXcell (IMV Technologies U.S.A., Maple Grove, MN, USA) and stored in liquid nitrogen for 2 months to 20 years. All samples were frozen using a dry shipper-based method [31,32], with differences limited to extender composition and the methodology used to extend the semen. Further protocol details are provided in the supplemental materials (Supplemental M&M and Supplemental Tables). In several cases, sperm from the same rhino collected on different days (at least one year apart) were used in experiments. The same procedure was utilized for thawing all semen: straws were removed from liquid nitrogen using forceps equilibrated to cryogenic temperature, wafted in air for 8–10 s, and then immersed in 37°C water for 20 s.

2.3. Sex-sorting experiments

2.3.1. Toll-like receptor activation

2.3.1.1. Immunofluorescence. To determine if TLR7 and TLR8 are expressed in rhino sperm, we performed immunofluorescence staining on frozen-thawed samples. Sperm were thawed, washed twice with phosphate-buffered saline (PBS), and resuspended in PBS containing Zombie Violet™ fixable dye (1:100; BioLegend, San Diego, CA, USA). After incubating sperm for 30 min at room temperature, an equal volume of PBS with 1 % bovine serum albumin (BSA-PBS) was added to stop the staining reaction. Samples were then centrifuged (600 g, 3 min), resuspended in PBS, and smeared onto uncoated glass microscope slides. Slides were fixed for 10 min in −20°C methanol (ACS grade, 100 %), air-dried, and stored at 4°C until further use.

For immunofluorescence staining, slides were blocked with BSA-PBST (0.1 % Tween 20; 1 h; RT) and then incubated overnight at 4°C with either 10 μg/mL of anti-TLR7 or 2 μg/mL anti-TLR8 in BSA-PBST (optimal antibody concentrations for specific signal relative to background noise were determined during initial experiments). Protein sequence alignment confirmed that the regions targeted by the antibodies for TLR7 and TLR8 shared ≥ 88 % sequence identity with the corresponding rhino TLR7 and TLR8 sequences available in GenBank (Supp Figs 1 & 2, respectively) [33]. For negative controls, additional slides were covered with BSA-PBST only. Slides were washed three times with PBS before incubating them with a 1:200 dilution of anti-rabbit IgG-AlexaFluor555 conjugate for 1 h at ambient temperature. For slides exposed to anti-TLR7, 20 μg/mL peanut agglutinin (PNA)-FITC conjugate was included with the detection antibody. After washing the slides three times with PBS, we mounted glass coverslips using Fluoromount™ aqueous medium. A 40X objective was used to evaluate the slides on a Zeiss Axioskop Fluorescent microscope equipped with an AxioCam 202 mono camera (Carl Zeiss Microscopy GmbH, Germany) and fluorescent filters for DAPI (excitation [ex.] 330–380 nm/emission [em.] 435–485 nm), GFP (ex. 465–495 nm/em. 515–555 nm) and TRITC (ex. 330–380 nm/em. 577–633 nm). We acquired images from the negative control and antibody-labeled slides at identical exposure settings and processed them using the same display adjustments within Zen 3.1 software (blue edition; Zeiss). For each slide, 3 – 10 fields of view were acquired to estimate the percentage of sperm staining positive for TLR7 and TLR8 and to assess localization. Immunofluorescence for TLR7 and TLR8 was performed on ten separate occasions using different straws of cryopreserved sperm from 4 different bulls (white, n = 2; GOH, n = 2).

2.3.1.2. TLR ligand treatment. Extended semen was washed with mEQ supplemented with 0.1 % poly(vinyl alcohol) [PVA; mol wt 10 K] and resuspended to a final concentration of 5–10 million sperm per milliliter (M/mL). Preliminary buffer testing revealed that frozen-thawed rhino sperm agglutinated when washed with modified Tyrode's medium (Sperm-TALP; [34])) or synthetic oviductal fluid, making these buffers unsuitable for use in this experiment (data not shown). We incubated sperm for 1 h at ambient temperature with various concentrations of a TLR8 ligand (0 – 30 μM Motolimod) in a 1 mL volume, then carefully pipetted the upper 0.5 mL (top) to separate it from the lower layer (bottom 0.5 mL; Fig. 1B). Each layer was evaluated on the iSperm device (Aidmics Biotechnology, Taipei City, Taiwan) for concentration, average path velocity, and total motility using the rhinoceros-specific software (beta ver. 5.3.50; [24]). Concentration values were used to calculate the proportion of total sperm present in the upper layer. Treated sperm were centrifuged (3000 g, 5 min), the supernatant discarded, and resulting pellets stored at −20°C until sex ratio determination. This experiment was repeated five times using sperm from two white (n = 3 cryopreserved) and two GOH (n = 1 fresh and n = 1 cryopreserved) rhinos.

2.3.2. Charged magnetic nanoparticles

2.3.2.1. Zeta potential measurement. Frozen-thawed semen from two different bulls (one each white and GOH rhino) was diluted 1:10 with one of six different media: two media known to be rhino sperm-friendly (mEQ, OptiXCell [23,24,26]) and four other media (CB, CM, TGC, and LHTF) used for sex-sorting sperm based on surface charge in other species [16,17,25], which differ in ionic composition (Supplemental M&M) and conductivity (Supp Table 3). We centrifuged the diluted sperm samples (600 g, 5 min) and resuspended the resulting sperm pellet in the corresponding diluting buffer to a final concentration of 5–15 M/mL. Sperm samples were loaded into a folded capillary zeta cell (DTS1070; prepared according to the manufacturer's instructions) and inserted into a Zetasizer Nano ZSP instrument (Malvern Panalytical Inc., GmbH, Kassel, Germany). We conducted four measurement runs at

ambient temperature for each cell (each sample was analyzed in duplicate) to derive the zeta potential (mV) of the sperm and the conductivity (mS/cm) of the buffer (Zetasizer Software, ver. 8.301.4906). We also assessed the surface charge of the 50 nm MNPs from Chemicell GmbH in various buffers (water, mHTF, mEQ, and OptiXcell extender) to determine if the MNPs would remain negatively charged when placed in different media.

2.3.2.2. MNP procedure. To optimize sperm-MNP interactions, different concentrations of MNPs were tested to identify conditions in which more than 30 % of sperm were associated with the nanoparticles (data not shown). Prior to incubation with sperm, the MNPs were diluted in 1 mL of either mEQ or mHTF, equilibrated for 30 min at ambient temperature with rocking, and then placed on a magnetic rack (DynaMag™-2; Thermo Fisher Scientific, Waltham, MA, USA). A tube without MNPs was included as a control to assess sperm under identical handling conditions without exposure to nanoparticles.

Meanwhile, sperm samples from both freshly collected (n = 5) and cryopreserved (n = 4) sources were washed with either mEQ or mHTF and resuspended to a final concentration of 80–100 M/mL. While the MNP-containing tubes remained on the magnetic rack, the supernatant was carefully removed to avoid disruption of the magnetically anchored nanoparticles. Sperm (0.5 mL) suspended in the matching medium was then added to each tube. Tubes were briefly removed from the rack and incubated for 5 min at ambient temperature with occasional gentle inversion to facilitate sperm-MNP interaction. The tubes were returned to the magnetic rack for 20 min to allow the sperm-MNP complexes to be pulled to the tube wall. The supernatant was carefully transferred to a new tube, i.e., the unbound fraction (Fig. 1C). To recover the presumed MNP-bound sperm, fresh buffer (0.5 mL) was added to the tubes and the contents were gently resuspended (Fig. 1C).

The concentration of sperm in the unbound fractions was assessed using the iSperm device and compared to the control samples (no MNP addition) to calculate the percentage of sperm that remained unbound after MNP incubation. The MNP-bound fractions were not evaluated because the presence of MNPs interfered with sperm concentration measurements. After iSperm assessment, all samples were centrifuged (3000 g, 5 min), the supernatant discarded, and the resulting pellets stored at −20°C for subsequent sex ratio determination. Preliminary testing indicated that approximately 5–10 % of the sperm remained in the control tubes after removal of the unbound fraction (data not shown). Both fractions of control samples were processed alongside the experimental groups for sex ratio analysis. The mEQ buffer experiment was repeated five times using sperm from three white rhinos (n = 4 fresh and n = 1 cryopreserved), whereas the mHTF experiment was repeated nine times using sperm from three white rhinos (n = 2 fresh and n = 3 cryopreserved) and two GOH rhinos (n = 1 fresh and n = 1 cryopreserved).

2.4. Determination of sex ratio in sorted samples

Total DNA was extracted from sperm using the GeneJET Genomic DNA Purification kit (Thermo Fisher) following the manufacturer's protocols for cultured mammalian cells, with modifications as described by Roth et al. [35]. A negative control (PBS buffer only) was used to check for extraneous DNA contamination during each extraction process. Nucleic acid concentration was measured using a Nanodrop-One (Thermo Fisher), and samples were diluted to 3 ng/μL using TE buffer (10 mM Tris-HCl, 0.1 mM EDTA, pH 8.0). For quality control, DNA was extracted from the tissues of male and female rhinos using the same DNA Purification kit [35].

To determine the sperm sex ratio, gene products for proteolipid protein 1 (PLP1, X chromosome) and sex-determining region on the Y chromosome (SRY) were amplified utilizing previously validated oligonucleotides (Table 1; [35]). All samples were run in duplicate, while controls and standards were run in triplicate. The ratio of X to Y chromosomes in each experimental sample was calculated using the following equations [20,36]: Percent X (%X) = X / (X + Y), Percent Y (% Y) = Y / (X + Y), and X:Y ratio = %X / %Y.

Table 1
Sequence of oligonucleotides used for sex ratio determination.

Gene	Descriptor	Sequence
PLP1	Forward primer	5'-GCTGCCACTTACAACTTTGC−3'
	Reverse primer	5'-AGGTTAGAGCCTCGCTATTAGA−3'
	Internal probe[a]	5'-**Sun**-CGTCCTTAA(**ZEN™**)ACTCATGGGCCGAGG-**IowaBlack®FQ**−3'
SRY	Forward primer	5'-ACCTTGGACTAGTAAGATAAGTTTCC−3'
	Reverse primer	3'-GTAATCATCGCTGCTAGATACCC−3'
	Internal probe[b]	5'-**FAM**-ACGGTGCCA(**ZEN™**)TCTTATGCTTCTGCT-**IowaBlack®FQ**−3'

Abbreviations: PLP1, proteolipid protein 1; SRY, sex-determining region for Y
[a] Probe modifications indicated in bold include a 5' fluorescent tag (SUN) and two dye-quenchers (internal ZEN™ tag and 3' Iowa Black tag)
[b] Probe modified to have a 5' fluorescent tag (6-FAM) and two dye-quenchers (internal ZEN™ tag and 3' Iowa Black tag)

For the TLR ligand samples, gene targets were amplified in separate reactions from a defined amount of sample, standard, or control. Standards consisted of purified X and Y amplification products that were mixed and serially diluted (10-fold) to five concentrations, ranging from 10^2 to 10^7 copies. Each 25 μL reaction contained 200 nM of each primer (forward and reverse), 1X PowerTrack+ ™ SYBR™ Green Master Mix (Applied Biosystems [ABI], Thermo Fisher), and 8 μL of sample, standard, or control. Thermal cycling was performed on a QuantStudio 3 real-time PCR system (ABI) using the following conditions: 50°C for 2 min, 95°C for 10 min, followed by 40 cycles of 95°C for 15 s and 58°C for 60 s (acquired fluorescence). Melt curve analysis was performed to confirm the specificity of the amplified products and the absence of primer dimers.

For the MNP samples, PLP1 and SRY targets were amplified together in a single reaction using TaqMan probes. The PCR reaction used the same component concentrations as those described by Roth et al. [35]; however, the thermocycling conditions were modified to accommodate quantitative analysis. Standards were prepared by mixing synthetic DNA for PLP1 and SRY (gBlocks® Gene Fragment synthesized by Integrated DNA Technologies, Coralville, IA, USA; Supp Figs 3 & 4) and serially diluting the mixture to seven concentrations, ranging from 10^3 to 10^7 copies. The thermocycling conditions were as follows: 95°C for 10 min, followed by 40 cycles at 95°C for 15 s, 58°C for 30 s (acquired fluorescence), and 72°C for 60 s.

2.5. Statistical analyses

Statistical modeling was performed using SAS 9.4 software (SAS Institute, Inc., Cary, NC, USA). Differences were designated significant for $P \leq 0.05$ and a tendency towards significance for $0.05 < P \leq 0.1$. Data were analyzed using a randomized block design with generalized linear mixed models (PROC GLIMMIX) with effects determined using an F-protected least significant difference test. The normality of data was evaluated using the Shapiro-Wilk test before assessing the statistical model results. No severe outliers or influential points were detected, and normality was deemed satisfactory for analyses ($W > 0.9$; Supp Table 1). Data are reported as least squares means ± SEM obtained using the inverse link option in SAS.

Differences in extender type and sperm origin (i.e., fresh versus frozen-thawed) were not included in the statistical analyses due to limited and unbalanced sample sizes across categories. The statistical model for the TLR experiment included fixed effects of TLR8 ligand

concentration (0 – 30 μM), layer (upper vs. lower), and their interaction with random effects of the date of the experiment and individual rhino as blocking factors. The main effect of ligand concentration was not reported for sperm concentration due to the interdependence of upper and lower fractions (values sum to 100 %). The statistical model for the MNP experiment varied based on the response variable. For sperm concentration analysis, only the unbound fractions from MNP-exposed groups were examined, as the control values were used to calculate the percentages. The model included treatment as a fixed effect (each combination of bead size and concentration assigned a unique treatment ID), with the date of the experiment and individual rhino as random blocking effects. For the sex ratio analysis, the model included fraction (unbound vs. MNP-bound) and its interaction with treatment (Bead Size*Conc) as fixed effects, with date of experiment and individual rhino included as random blocking factors. Analyses were conducted separately for each buffer type (mEQ and mHTF). The main effect of treatment was not interpreted independently, as its biological relevance is contingent upon differences between the paired fractions.

3. Results and discussion

3.1. Toll-like receptor activation

3.1.1. Localization of TLR7 and TLR8

Immunofluorescence staining confirmed the presence of TLR7 and TLR8 in rhino sperm (Fig. 2). Negative controls (sperm exposed only to the detection antibody) exhibited no detectable AlexaFluor555 staining (Fig. 2A). A consistent expression pattern was observed across samples, with TLR7 primarily localized to the sperm head (90–95 %; Fig. 2B) and TLR8 predominantly found on the flagellum (~50 %; Fig. 2C). TLR7 staining appeared to be associated with the acrosomal cap, as staining was absent in the upper head region of sperm lacking an intact acrosomal membrane. However, TLR7 staining in the lower area of the head persisted in all sperm, regardless of plasma membrane integrity (Fig. 2B). These findings align with those of Pan et al. [37], who reported that TLR7 was expressed in all observed canine sperm (head and tail regions). In contrast, others have reported TLR7 expression in only half of the population of bovine [38], caprine [17], and murine sperm [20].

Staining for TLR8 was localized to the flagellum and in the equatorial head region of rhino sperm. Notably, TLR8 expression on the flagellum was observed, regardless of plasma membrane integrity (Fig. 2C). Although the expression pattern varied slightly, previous studies have reported TLR8 localization to the flagella of approximately half of the sperm population (bovine: [19]; caprine: [17]). The disparities in the observed expression patterns for both TLRs may be species-specific, although technical differences in immunofluorescence protocols (e.g., antibody targets) or sperm processing (e.g., fresh versus frozen, washed versus swim-up, etc.) could also underlie the different findings across studies. Variability in the staining patterns within the same species has also been reported. Zhao et al. [39] observed that 100 % of murine and bovine sperm were positive for TLR7 expression, whereas others have described TLR7 to be present in only 50 % of the population [19,20,38]. These inconsistencies highlight the potential influence of methodological differences on receptor detection, localization, and activation.

3.1.2. Sex-sorting with TLR8 ligand

Given that TLR7 was predominantly localized to the sperm head and that nearly all rhino sperm expressed this receptor, a ligand specific for TLR8 (motolimod) was selected to test the sex-sorting procedure described by Umehara et al. [20]. This method relies on TLR7/8 activation to reduce the motility of X-bearing sperm, stimulating the more motile Y-bearing cells to be in the upper layer and the less motile X-bearing sperm in the lower layer (Fig. 1B). Exposure to the TLR8 ligand had no significant impact on the distribution of sperm between the upper and lower swim-up fractions (TLR8 x Layer interaction, Concentration $P = 0.6942$; Table 2). Sperm velocity (i.e., swimming speed) trended differently between layers depending on TLR8 agonist concentration (TLR8 x Layer interaction, VAP $P = 0.0719$; Table 2). This trend arose from two findings: first, the highest ligand concentration reduced the overall swimming speed (TLR8 Ligand, VAP $P = 0.0010$), and second, sperm in the upper layer swam slower than their lower-layer counterparts (Layer Location, VAP $P < 0.0001$; Table 2). The observed reduction in sperm velocity following TLR8 ligand treatment was consistent with previous findings that TLR activation affects sperm motility. Whether the same mechanisms observed in other species, particularly the suppression of mitochondrial ATP generation via hexokinase signaling pathways [17,20,38,40], were also affected in rhino sperm remains to be determined.

Although TLR8 ligand exposure reduced sperm velocity, it did not significantly affect the proportion of motile sperm in either layer (TLR8 x Layer interaction and TLR8 Ligand, Motile $P > 0.05$; Table 2). Regardless of treatment, the lower layer consistently contained a higher proportion of motile sperm than the upper layer (Layer Location, Motile $P < 0.0001$; Table 2). These results contrast with previous reports in which TLR activation caused a shift of the slower swimming sperm to the

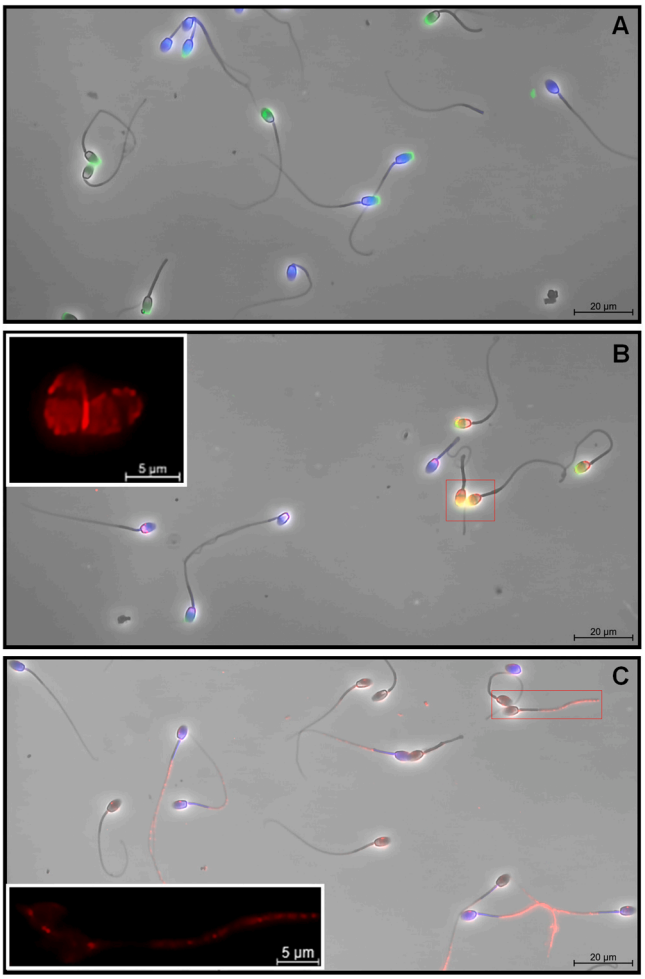

Fig. 2. Immunofluorescent localiztion of toll-like receptors 7 and 8 on rhinoceros sperm.Rhinoceros sperm were pre-stained with Zombie Violet (viability stain; depicted in blue) before mounting and methanol fixation. Afterward, samples were incubated with toll-like receptor (TLR) antibodies (shown in red). In some instances, the acrosomal membranes were stained with peanut agglutinin (green staining). Co-localization of TLR staining with Zombie violet appears violet, whereas the overlap of TLR7 with acrosomal staining appears yellow. Representative images include A) Negative control (no primary antibody), B) TLR7 localization, and C) TLR8 localization. Boxes indicate the area shown in the inset, which is a magnified view showing only the TLR staining pattern.

Table 2
Effect of toll-like receptor 8 (TLR8) ligand concentration on distribution and mobility characteristics of rhinoceros sperm in upper and lower layers after 1 h incubation.

		Concentration[a] (%)	VAP[2] (μm/s)	Motile[3] (%)
TLR8 ligand			*P = 0.0010*	*P = 0.1827*
0 μM		n.a.	27.22 ± 6.1 [A]	30.84 ± 15.5
0.03 μM		n.a.	24.89 ± 6.2 [A]	33.22 ± 15.5
0.3 μM		n.a.	26.56 ± 6.2 [A]	31.75 ± 15.5
3 μM		n.a.	27.50 ± 6.2 [A]	32.79 ± 15.5
30 μM		n.a.	18.44 ± 6.2[B]	26.22 ± 15.6
Layer Location		*P < 0.0001*	*P < 0.0001*	*P < 0.0001*
Upper		41.74 ± 1.5[B]	20.50 ± 6.1[B]	23.88 ± 15.5[B]
Lower		58.26 ± 1.5 [A]	29.34 ± 6.1 [A]	38.05 ± 15.5 [A]
TLR8 ligand x Layer		*P = 0.6942*	*P = 0.0719*	*P = 0.1427*
0 μM	Upper	40.66 ± 2.4	21.19 ± 6.2	21.55 ± 15.5
	Lower	59.34 ± 2.4	33.25 ± 6.2	40.13 ± 15.5
0.03 μM	Upper	40.41 ± 3.4	21.22 ± 6.3	24.60 ± 15.6
	Lower	59.59 ± 3.4	28.57 ± 6.3	41.84 ± 15.6
0.3 μM	Upper	40.59 ± 3.4	23.65 ± 6.3	22.83 ± 15.6
	Lower	59.41 ± 3.4	29.46 ± 6.3	40.67 ± 15.6
3 μM	Upper	42.24 ± 3.4	20.01 ± 6.3	27.26 ± 15.6
	Lower	57.76 ± 3.4	34.90 ± 6.3	38.32 ± 15.6
30 μM	Upper	44.80 ± 3.8	16.36 ± 6.4	23.14 ± 15.7
	Lower	55.20 ± 3.8	20.53 ± 6.4	29.31 ± 15.7

Data associated with this table can be found in supplemental tables file.
n.a. = not applicable; see statistical analysis section for explanation
[a] Percent of total sperm recovered; [2]Average path velocity (μm/s); [3]Percent of sperm with a VAP > 5 μm/s. [A-B]For each effect where $P \leq 0.05$, the means within the same column that do not share a superscript letter differ significantly.

lower layer [17,19,20,37,38]. Similarly, we did not observe a selective effect on X-bearing sperm; the ratio of X- to Y-bearing sperm remained approximately 50:50 in both layers, regardless of treatment (P > 0.05; Fig. 3). Our findings align with those of Pan et al. [37], who reported slower swimming velocity but no sex-ratio differences in canine sperm following activation with resiquimod (R848), a ligand that activates both TLR7 and TLR8.

Several factors may explain why the sex-sorting effect was not observed with the rhino sperm. It is possible that motolimod does not activate rhino TLR8 in the same manner as resiquimod, which selectively affects X-bearing sperm motility in other species [17,19,37,41]. Although the TLR8 protein is highly conserved across mammalian species, variations in the ligand binding sites may lead to species-specific functional responses. For instance, the human TLR7-specific agonist imiquimod (R837) has been shown to activate both porcine TLR7 and

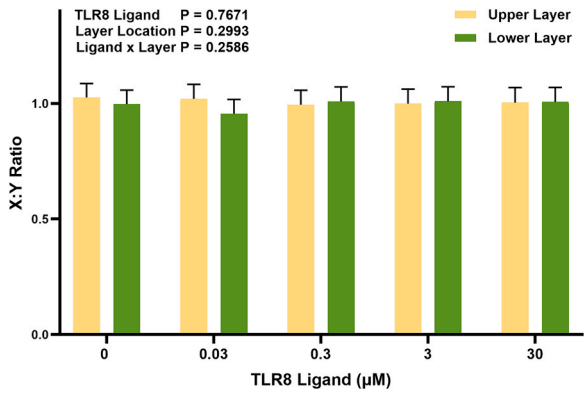

Fig. 3. Effect of toll-like receptor 8 (TLR8) ligand on distribution of X-bearing sperm. The ratio of X to Y-bearing sperm in each layer (upper layer, lower layer) after incubating rhinoceros sperm for 1 h with varying concentrations of motolimod (VTX-378), a ligand specific for TLR8. Data associated with this figure can be found in the supplemental tables file.

TLR8 [42]. To date, the effects of motolimod on TLRs have only been examined in human and mouse cells [43], and its ability to activate rhino TLR8 may differ. The metabolic substrate within the buffer also may have influenced our results. The TLR-mediated sorting mechanism relies on selectively disrupting ATP production via the hexokinase pathway (i.e., glycolysis) and requires an optimal glucose concentration to function effectively. Umehara and others (2020; [19]) demonstrated that for mouse sperm, a glucose concentration of 2 mM promoted X-Y sperm separation, whereas media containing either 0 mM or 10 mM glucose resulted in less than 10 % of the total sperm in the upper layer under control conditions. While the absolute concentrations differ, our preliminary buffer testing revealed a similar pattern for rhino sperm: media containing 0 and 1.67 mM glucose resulted in little to no sperm within the upper layer, whereas the buffer used for the experiments (mEQ) – containing 76 mM glucose – resulted in ~43 % of the total sperm in the upper layer. Concentrations higher than 76 mM were not tested; therefore, the upper limit of glucose required to support optimal motility for the separation of rhino sperm remains unknown.

Although the preferred metabolic pathways in rhino sperm remain uncharacterized, metabolic differences between species may partly explain why higher glucose concentrations were required to support sperm remaining in the upper layer. In stallion sperm, motility can be sustained by glucose alone, but mitochondrial function may be impaired in the absence of other substrates such as lactate or pyruvate [44,45]. Additional research is needed to determine whether modifying energy substrate composition or selecting an alternative ligand could improve the effectiveness of TLR-mediated sorting in rhino sperm.

3.2. Charged magnetic nanoparticles

3.2.1. Zeta potential

The zeta potential (ZP; aka surface charge) of rhino sperm measured in six different buffers varied with the average ZP ranging from −26.7 to −10.6 mV (Supp Table 3). This fluctuation was expected, as zeta potential is strongly influenced by salt concentration, ionic strength, and the pH of the suspension medium. The range of ZP values observed was largely consistent with those reported for other species. For example, the ZP values of rhino sperm in the chamber buffer ranged from −31 to −12 mV, which aligns with the reported values for human sperm in the same buffer (-22 to −14 mV; [23]). However, unlike human sperm, which display two distinct ZP peaks [23], rhino sperm exhibited a continuous distribution of values (Supp Fig 5), a pattern more consistent with previous findings in bovine sperm [46]. The absence of two distinct peaks in our study is not necessarily problematic, as bovine sperm have been successfully sorted by surface charge using electrophoretic techniques [22,29].

We also assessed the surface charge of magnetic nanoparticles under various buffer conditions as MACS relies on negatively charged nanoparticles to selectively associate (i.e., bind) with the presumed more positively charged Y-bearing sperm, thereby enriching the unbound fraction with X-bearing sperm (Fig. 1C). Magnetic nanoparticles retained their negative charge when placed in mEQ (mean ZP = −25.2 mV) and mHTF (mean ZP = −26.1 mV; Supp Table 4). However, in OptiXcell extender, they exhibited a shift toward a more positive charge (mean ZP = −2.9 mV; Supp Table 4), which would likely interfere with their ability to selectively associate with Y-bearing sperm. This finding suggests that OptiXcell would be unsuitable for the enrichment of X-bearing sperm via the MACS method.

3.2.2. Sex-sorting with charged MNPs

These experiments were conducted as proof of concept to evaluate if MNPs could be used to selectively enrich for X-bearing sperm. The primary focus was on assessing sperm distribution and sex ratio outcomes rather than evaluating the potential effects of MNP exposure on sperm quality. The percentage of sperm remaining in the unbound fraction significantly varied based on bead size and concentration across both

buffer types. In mEQ buffer, the percentage of sperm remaining in the unbound fraction ranged from 55.28 % to 79.5 % (Bead Size*Conc, P = 0.0154; Supp Table 5), whereas in mHTF buffer, approximately half of the sperm remained unbound following incubation with the MNPs (range 36–56 %; Bead Size*Conc, P = 0.0361; Supp Table 6). These differences were expected, as the MNP concentrations were selected to result in at least 30 % of the sperm associating with the MNPs, consistent with previous studies utilizing negatively charged nanoparticles for sex-sorting [24–26].

For the sex ratio analysis, no significant differences were observed across treatment conditions in either fraction when using either mEQ or mHTF media (Bead x Fraction interaction, P > 0.05; Fig. 4). Therefore, the effects of the fraction were evaluated independently. In mEQ, there was a tendency for the unbound fraction to contain more Y-bearing sperm (X:Y ratio = 0.978 ± 0.01) compared to the MNP-bound fraction (X:Y ratio = 1.016 ± 0.01), regardless of treatment conditions (Fraction, P = 0.0667; Fig. 4A). However, the observed differences in sex ratio were minimal, less than a 1 % shift in the amount of X-bearing sperm, and are unlikely to have biological relevance. In mHTF, no significant differences in sex ratio were detected between fractions (Fraction, P = 0.9301; Fig. 4B). With both media, a small number of sperm were recovered from the 'MNP-bound' fraction in control tubes lacking MNPs, likely due to water tension or non-specific adherence to the tube surface. Such nonspecific retention may also account for a portion of the sperm recovered in the MNP-bound fractions from treated samples. However, the consistency of low skewing across treatments within each fraction and the minimal overall shift in sex ratio suggest that this contribution was negligible.

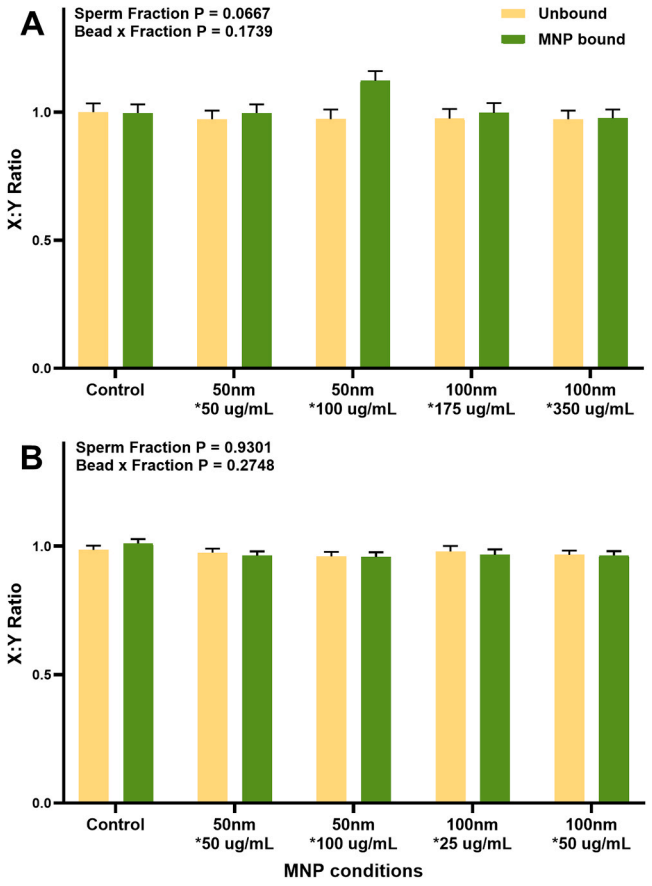

Fig. 4. Effect of magnetic nanoparticle (MNP) exposure on the sex ratio of rhinoceros sperm.Sex ratio (X:Y Ratio) was assessed in both unbound and MNP-bound sperm fractions following incubation in (A) modified equine extender and (B) modified Human Tubal Fluid. Data associated with this figure can be found in the supplemental tables file.

Despite achieving sperm association with MNPs, the expected enrichment of X-bearing sperm in the unbound fraction was not observed. This result contrasts with a previous study on donkey sperm, which reported enriching for X-bearing sperm with a 90 % efficiency [24]. The discrepancy could be due to the difference in how the sex ratio of the sorted population was assessed; Dominguez et al. [24] relied on a shift in the average fluorescent intensity in the sperm population as detected by flow cytometry, whereas we quantified the number of X and Y chromosomes. Although we did not observe that MNP exposure physically separated sperm based on sex chromosome content, it is possible that it could have selectively affected the fertilization potential of the Y-bearing sperm, as suggested by Naar-Esfahani et al. [47]. Human sperm subjected to selection based on zeta potential using a charged tube instead of MNPs resulted in more female babies compared to the non-sorted sperm (63.6 % vs. 38.5 %, respectively) without a significant change in the ratio of X to Y-bearing sperm [47]. This finding could explain why horse sperm sorted using charge MNPs and then used for AI resulted in 95 % of the pregnancies being female, as confirmed by ultrasound [25]. In vitro fertilization with MNP-sorted rhino sperm would be necessary to determine whether a similar effect occurs, but this is not currently feasible due to the significant financial and biological resource investment required [48].

4. Conclusions

Although we conclusively demonstrated the presence of TLR7 and TLR8 in rhino sperm and recorded similar surface charges for rhino sperm as reported for other species, we were not successful in using these characteristics to sort X- from Y-bearing cells. However, there are numerous potentially confounding factors, as discussed, and the impacts of methodologies should not yet be ruled out. Further research to better understand the fundamental physiology of rhino sperm could be valuable in designing protocol modifications more conducive to effectively sorting their sperm via these innovative methodologies. This study highlights both the potential and the challenges associated with alternative sperm sex-sorting techniques and provides valuable insights into the physiological and methodological factors that must be considered when optimizing sex-sorting strategies.

CRediT authorship contribution statement

Louisa A. Rispoli: Writing – original draft, Visualization, Methodology, Investigation, Funding acquisition, Formal analysis, Data curation, Conceptualization. **Elizabeth Donelan:** Writing – review & editing, Methodology, Investigation. **Parker M. Pennington:** Writing – review & editing, Methodology, Investigation, Conceptualization. **Priscilla H. Joyner:** Writing – review & editing, Resources, Investigation. **Terri L. Roth:** Writing – review & editing, Supervision, Funding acquisition, Conceptualization.

Declaration of Generative AI and AI-assisted technologies in the writing process

During the preparation of this work, the corresponding author used Grammarly to improve the readability and language of the manuscript and iThenticate (Turnitin, LLC) to check for unoriginal work. After using these tools, the author reviewed and edited the content as needed and takes full responsibility for the content of the published article.

Funding

This work was supported by the Institute of Museum and Library Services [grant # MG-249011-OMS-21: "The American Institute of Rhinoceros Science (AIRS) – A Model for Saving Species with Science ex situ"], the Basis Endowment Foundation, and by generous gifts from Tucker and Michael Coombe and Elizabeth Tu Hoffman.

Declaration of Competing Interest

The authors declare the following financial interests/personal relationships which may be considered as potential competing interests, Terri L. Roth reports financial support was provided by Institute of Museum and Library Services. Louisa A. Rispoli reports financial support was provided by The Basis Endowment Foundation. Terri L. Roth reports financial support was provided by Tucker and Michael Coombe. Terri L. Roth reports financial support was provided by Elizabeth Tu Hoffman. If there are other authors, they declare that they have no known competing financial interests or personal relationships that could have appeared to influence the work reported in this paper.

Acknowledgements

The authors thank the many zoos and rhino holding facilities for their willingness to collaborate and contribute samples for research. Specifically, we thank Buffalo Zoo, Fossil Rim Wildlife Center, Lion Country Safari, Los Angeles Zoo and Botanical Garden, Rolling Hills Zoo, The Wilds, and White Oak Conservation for their contributions to this effort.

Appendix A. Supporting information

Supplementary data associated with this article can be found in the online version at doi:10.1016/j.therwi.2025.100135.

References

[1] C. Ververs, M. Van Zijll Langhout, M. Hostens, M. Otto, J. Govaere, B. Durrant, et al., Reproductive performance parameters in a large population of game-ranched white rhinoceroses (*Ceratotherium simum simum*), PLoS One 12 (2017) e0187751, https://doi.org/10.1371/JOURNAL.PONE.0187751.

[2] K. Carlstead, J. Fraser, C. Bennett, D.G. Kleiman, Black rhinoceros (*Diceros bicornis*) in U.S. Zoos: II. Behavior, breeding success, and mortality in relation to housing facilities, Zoo. Biol. 18 (1999) 35–52, https://doi.org/10.1002/(SICI)1098-2361(1999)18:1<35::AID-ZOO5>3.0.CO;2-L.

[3] Smith L., Kutilek C., Toman A., Ferrie G. Eastern black rhinoceros (*Diceros bicornis michaeli*). AZA Species Survival Plan® Signature Program Population Analysis and Breeding and Transfer Plan. Chicago, IL: 2025.

[4] Eyres A., Beetem D., Capiro J., Ivy J. Southern White Rhinoceros (*Ceratoterium simum simum*). AZA Species Survival Plan® Signature Program Population Analysis and Breeding and Transfer Plan. Chicago, IL: 2025.

[5] Wade S., Cseplo C., Ivy J. Greater One-Horned Rhinoceros (*Rhinoceros unicornis*). AZA Species Survival Plan® Signature Program Population Analysis and Breeding and Transfer Plan. Chicago, IL: 2025.

[6] L.C. Metrione, A. Eyres, S. Shurter, S. Ellis, T.L. Roth, W. Shaffstall, et al., Rhino Husbandry Manual, International Rhino Foundation, Fort Worth, TX, 2014.

[7] T.B. Hildebrandt, R. Hermes, F. Goeritz, R. Appeltant, S. Colleoni, B. de Mori, et al., The ART of bringing extinction to a freeze – history and future of species conservation, exemplified by rhinos, Theriogenology 169 (2021) 76–88, https://doi.org/10.1016/j.theriogenology.2021.04.006.

[8] I. Lueders, W.R.T. Allen, Managed wildlife breeding-an undervalued conservation tool? Theriogenology 150 (2020) 48–54, https://doi.org/10.1016/j.theriogenology.2020.01.058.

[9] J.K. O'Brien, K.J. Steinman, T.R. Robeck, Application of sperm sorting and associated reproductive technology for wildlife management and conservation, Theriogenology 71 (2009) 98–107, https://doi.org/10.1016/j.theriogenology.2008.09.052.

[10] J.K. O'Brien, T.L. Roth, M.A. Stoops, R.L. Ball, K.J. Steinman, G.A. Montano, et al., Sperm sex-sorting and preservation for managing the sex ratio and genetic diversity of the southern white rhinoceros (*Ceratotherium simum simum*), Anim. Reprod. Sci. 152 (2015) 137–153, https://doi.org/10.1016/j.anireprosci.2014.11.016.

[11] O'Brien J.K., Stoops M.A., Roth T.L., Ball R.L., Montano G.A., Steinman K.J., et al. Progress in sperm sorting and cryopreservation technologies for modifying population sex ratio and preserving genetic diversity in the rhinoceros and elephant. Scientific Program of the 15th International Elephant & Rhino Conservation and Research Symposium, Singapore: 2016.

[12] B. Behr, D. Rath, P. Mueller, T.B. Hildebrandt, F. Goeritz, B.C. Braun, et al., Feasibility of sex-sorting sperm from the white and the black rhinoceros (*Ceratotherium simum, Diceros bicornis*), Theriogenology 72 (2009) 353–364, https://doi.org/10.1016/J.THERIOGENOLOGY.2009.03.001.

[13] G.E. Seidel, Update on sexed semen technology in cattle, Animal 8 (2014) 160–164, https://doi.org/10.1017/S1751731114000202.

[14] S.P. De Graaf, T. Leahy, R. Vishwanath, Biological and practical lessons associated with the use of sexed semen, 8:bp008rdr35, Biosci. Proc. (2019), https://doi.org/10.1530/biosciprocs.8.035.

[15] P.A. Navarro-Costa, A. Molaro, C.S. Misra, C.D. Meiklejohn, P.J. Ellis, Sex and suicide: the curious case of Toll-like receptors, PLoS Biol. 18 (2020) e3000663, https://doi.org/10.1371/JOURNAL.PBIO.3000663.

[16] F. Wen, W. Liu, Y. Li, Q. Zou, M. Xian, S. Han, et al., TLR7/8 agonist (R848) inhibit bovine X sperm motility via PI3K/GSK3α/β and PI3K/NFκB pathways, Int. J. Biol. Macromol. 232 (2023) 123485, https://doi.org/10.1016/J.IJBIOMAC.2023.123485.

[17] F. Ren, H. Xi, Y. Ren, Y. Li, F. Wen, M. Xian, et al., TLR7/8 signalling affects X-sperm motility via the GSK3 α/β-hexokinase pathway for the efficient production of sexed dairy goat embryos, J. Anim. Sci. Biotechnol. 12 (2021) 89, https://doi.org/10.1186/s40104-021-00613-y.

[18] R. Setiawan, R. Widyastuti, A.A. Nurmeidiansyah, N. Solihati, The effect of Toll-like receptor 7/8 ligand in inhibiting the motility of putative X-chromosome-bearing sperm in rams, –648, J. Adv. Vet. Anim. Res. 11 (2024) 648, https://doi.org/10.5455/JAVAR.2024.K814.

[19] T. Umehara, N. Tsujita, Z. Zhu, M. Ikedo, M. Shimada, A simple sperm-sexing method that activates TLR7/8 on X sperm for the efficient production of sexed mouse or cattle embryos, Nat. Protoc. 15 (2020) 2645–2667, https://doi.org/10.1038/s41596-020-0348-y.

[20] T. Umehara, N. Tsujita, M. Shimada, Activation of Toll-like receptor 7/8 encoded by the X chromosome alters sperm motility and provides a novel simple technology for sexing sperm, PLoS Biol. 17 (2019) 1–24, https://doi.org/10.1371/journal.pbio.3000398.

[21] S. Kaneko, S. Oshio, T. Kobayashi, R. Iizuka, H. Mohri, Human X- and Y-bearing sperm differ in cell surface sialic acid content, Biochem Biophys. Res. Commun. 124 (1984) 950–955, https://doi.org/10.1016/0006-291X(84)91050-7.

[22] T. Wongtawan, N. Dararatana, B. Onnkhanond, S. Kornmatissuk, B. Oonkhanond, S. Kornmatissuk, Zeta potential of bovine X and Y sperm and its application for sperm sorting, Thai J. Vet. Med. 48 (2018). O25–6.

[23] S.A. Ishijima, M. Okuno, H. Mohri, Zeta potential of human X- and Y-bearing sperm, Int J. Androl. 14 (1991) 340–347, https://doi.org/10.1111/j.1365-2605.1991.tb01102.x.

[24] E. Domínguez, A. Moreno-Irusta, H.R. Castex, A.F. Bragulat, C. Ugaz, H. Clemente, et al., Sperm sexing mediated by magnetic nanoparticles in donkeys, a preliminary in vitro study, J. Equine Vet. Sci. 65 (2018) 123–127, https://doi.org/10.1016/j.jevs.2018.04.005.

[25] H.R. Castex, Losinno luis, Magnetic nanoparticles for X sperm separation from equine semen. Field and commercial results, CES Med. Vet. Y. Zootec. 2 (2018) 268–275.

[26] M. Moradi, H. Hajarian, H. Karamishabankareh, L. Soltani, B. Soleymani, Recovery of sperms bearing X chromosomes with different concentrations of magnetic nanoparticles in ram, Reprod. Domest. Anim. 56 (2020) 263–269, https://doi.org/10.1111/rda.13807.

[27] M.A. Stoops, M.K. Campbell, C.J. Dechant, J. Hauser, J. Kottwitz, R.D. Pairan, et al., Enhancing captive Indian rhinoceros genetics via artificial insemination of cryopreserved sperm, Anim. Reprod. Sci. 172 (2016) 60–75, https://doi.org/10.1016/j.anireprosci.2016.07.003.

[28] L.A. Rispoli, T.L. Roth, Validation of the iSperm for assessing rhinoceros sperm, Theriogenology Wild 3 (2023) 100048, https://doi.org/10.1016/J.THERWI.2023.100048.

[29] T. Wongtawan, N. Dararatana, C. Thongkittidilok, S. Kornmatitsuk, B. Oonkhanond, Enrichment of bovine X-sperm using microfluidic dielectrophoretic chip: a proof-of- concept study, Heliyon 6 (2020) e05483, https://doi.org/10.1016/j.heliyon.2020.e05483.

[30] R. Ma, C. Han, Z. Sun, G. Huang, Z. Yu, Y. Zhou, et al., A low conductivity culture medium suitable for the evaluation of sperm motility. Seventh International Conference on Photonics and Imaging in Biology and Medicine, SPIE, 2009, pp. 141–147, vol. 7280 http://10.1117/12.822761.

[31] T.L. Roth, L.M. Bush, D.E. Wildt, R.B. Weiss, Scimitar-Horned Oryx (*Oryx dammah*) spermatozoa are functionally competent in a heterologous bovine in vitro fertilization system after cryopreservation on dry ice, in a dry shipper, or over liquid nitrogen vapor, Biol. Reprod. 60 (1999) 493–498, https://doi.org/10.1095/BIOLREPROD60.2.493.

[32] J. Wojtusik, M.A. Stoops, T.L. Roth, Animal protein-free OptiXcell and shortened equilibration periods can replace egg yolk-based extender and slow cooling for rhinoceros semen cryopreservation, Cryobiology 89 (2019) 21–25, https://doi.org/10.1016/j.cryobiol.2019.06.003.

[33] E.W. Sayers, E.E. Bolton, J.R. Brister, K. Canese, J. Chan, D.C. Comeau, et al., Database resources of the National Center for Biotechnology Information, Nucleic Acids Res. 50 (2021) D20, https://doi.org/10.1093/NAR/GKAB1112.

[34] J.J. Parrish, J. Susko-Parrish, M.A. Winer, N.L. First, Capacitation of bovine sperm by heparin, Biol. Reprod. 38 (1988), https://doi.org/10.1095/biolreprod38.5.1171.

[35] T.L. Roth, S.L. Rebolloso, E.M. Donelan, L.A. Rispoli, J.P. Buchweitz, Rhinoceros horn mineral and metal concentrations vary by sample location, depth, and color, 2024;14:1–13, Sci. Rep. 14 (1) (2024), https://doi.org/10.1038/s41598-024-64472-z.

[36] A.F. Maleki, A.R.H. Moussavi, M.R. Nassiri, M. Tahmoorespur, S.A. Vakili, Introducing and validation of SYBR Green Real-Time PCR method to determinate sex ratio in bovine semen, Anim. Reprod. Sci. 140 (2013) 1–6, https://doi.org/10.1016/j.anireprosci.2013.05.009.

[37] C. Pan, S. Xu, W. Zhang, Y. Zhao, J. Zhao, M. Song, Expression of TLR7/8 in canine sperm and evaluation of the effect of ligand R848 on the sorting of canine X/Y

sperm, Theriogenology 231 (2025) 127–132, https://doi.org/10.1016/J.THERIOGENOLOGY.2024.10.015.
[38] F. Wen, W. Liu, Y. Li, Q. Zou, M. Xian, S. Han, et al., TLR7/8 agonist (R848) inhibit bovine X sperm motility via PI3K/GSK3α/β and PI3K/NFκB pathways, Int. J. Biol. Macromol. 232 (2023) 123485, https://doi.org/10.1016/J.IJBIOMAC.2023.123485.
[39] R. Zhao, J. Liu, B. Wang, X. Tian, 142 Evidence against the role of Toll-like receptors 7/8 in sex selection in the mouse, Reprod. Fertil. Dev. 36 (2023) 224, https://doi.org/10.1071/RDV36N2AB142.
[40] X. Zhu, D. Shi, X. Li, W. Gong, F. Wu, X. Guo, et al., TLR signalling affects sperm mitochondrial function and motility via phosphatidylinositol 3-kinase and glycogen synthase kinase-3α, Cell Signal 28 (2016) 148–156, https://doi.org/10.1016/j.cellsig.2015.12.002.
[41] S. Yotov, D. Abadjieva, A. Atanasov, B. Ivanova, P. Taushanova, I. Fasulkov, et al., In vitro characteristics of X- and Y-bearing ram spermatozoa sorted by bovine serum albumin (BSA) column and TLR7/8 ligand R848, Anim. Reprod. Sci. 263 (2024) 107450, https://doi.org/10.1016/J.ANIREPROSCI.2024.107450.
[42] J. Zhu, K. Lai, R. Brownile, L.A. Babiuk, G.K. Mutwiri, Porcine TLR8 and TLR7 are both activated by a selective TLR7 ligand, imiquimod, Mol. Immunol. 45 (2008) 3238–3243, https://doi.org/10.1016/J.MOLIMM.2008.02.028.
[43] G. Frega, Q. Wu, J. Le Naour, E. Vacchelli, L. Galluzzi, G. Kroemer, et al., Trial Watch: experimental TLR7/TLR8 agonists for oncological indications, Oncoimmunology 9 (2020) 1796002, https://doi.org/10.1080/2162402X.2020.1796002.
[44] C.R. Darr, D.D. Varner, S. Teague, G.A. Cortopassi, S. Datta, S.A. Meyers, Lactate and pyruvate are major sources of energy for stallion sperm with dose effects on mitochondrial function, motility, and ROS production, Biol. Reprod. 95 (2016), https://doi.org/10.1095/BIOLREPROD.116.140707/2883430.
[45] F.J. Peña, F.E. Martín-Cano, L. Becerro-Rey, E. da Silva-Álvarez, G. Gaitskell-Phillips, C. Ortega-Ferrusola, et al., Reimagining stallion sperm conservation: combating carbotoxicity through pyruvate-induced Warburg effect to enhance sperm longevity and function, J. Equine Vet. Sci. 143 (2024) 105204, https://doi.org/10.1016/J.JEVS.2024.105204.
[46] V. Magdanz, J. Gebauer, P. Sharan, S. Eltoukhy, D. Voigt, J. Simmchen, Sperm-particle interactions and their prospects for charge mapping, Adv. Biosyst. 3 (2019), https://doi.org/10.1002/adbi.201900061.
[47] M.H.N. Esfahani, M.R. Deemeh, M. Tavalaee, M.H. Sekhavati, H. Gourabi, Zeta sperm selection improves pregnancy rate and alters sex ratio in male factor infertility patients: a double-blind, randomized clinical trial, Int. J. Fertil. Steril. 10 (2016) 253–260, https://doi.org/10.22074/IJFS.2016.4917.
[48] T.B. Hildebrandt, S. Holtze, S. Colleoni, R. Hermes, J. Stejskal, I. Lekolool, et al., In vitro fertilization program in white rhinoceros, Reproduction 166 (2023) 383–399, https://doi.org/10.1530/REP-23-0087/VIDEO-2.